

# Thermal Stability of $(\text{Mg}/\text{NbO}_x)_{82}$ Multilayer Nanostructure

Oleg Stognei,\* Andrey Smirnov, Alexander Sitnikov, and Mikhail Volochaev

Thermal stability of the multilayer  $(\text{Mg}/\text{NbO}_x)_{82}$  nanostructure and the effect of heat treatment on its electrical properties and phase composition depending on the bilayer thickness are studied. The studied  $(\text{Mg}/\text{NbO}_x)_{82}$  samples contain 82 bilayers whose thickness varies in the range from 2.2 to 6.2 nm. The  $\text{NbO}_x$  layer thickness in the multilayers is the same (0.96 nm) in all samples, while the magnesium layers thickness is varied. It is established that the magnesium layers are either discrete (a set of nanosized particles) or continuous depending on their thickness. A metallothermic reaction occurs in  $(\text{Mg}/\text{NbO}_x)_{82}$  multilayer nanostructures at a temperature of 430 °C: niobium oxide decomposes and the released oxygen partly oxidizes the magnesium layers. That leads to the conductive magnesium metal layers breaking and to the sharp increase of the nanostructures' resistance by more than two orders. Despite the metallothermic reaction, the layering of the  $(\text{Mg}/\text{NbO}_x)_{82}$  nanostructures as a whole and the presence of unoxidized magnesium inclusions remain even after heating up to 450 °C.

effect increases significantly.<sup>[17]</sup> Therefore, the hydrogen sorption–desorption processes in materials formed by nanocrystalline magnesium and niobium oxide are being investigated actively.<sup>[10,11,18]</sup>

Mainly, the research objects are powder composites obtained by mechanical milling in vacuum or argon to avoid the magnesium oxidation.<sup>[15,16,19,20]</sup> On the other hand, multilayer structures with nanosized layers are alternative structures to powder composites.<sup>[21]</sup> The structures formed from different materials are being studied within this direction: metal–metal systems ( $\text{Mg}/\text{Ni}$ ,<sup>[22]</sup>  $\text{Mg}/\text{Pd}$ <sup>[23]</sup>) as well as metal–oxide systems ( $\text{Ti}/\text{TiO}_2$ <sup>[24]</sup>). It should be noted that the catalyst in multilayer systems plays the same important role as it does in the powder composites,<sup>[22,23,25]</sup> therefore, the obvious interest is paid to multilayer nanostructures formed by niobium oxide

## 1. Introduction


Magnesium is one of the main elements which is used to create a material for hydrogen reversible storage in a form of solid-state hydrides.<sup>[1,2]</sup> The problem limiting the magnesium hydrides use is their high stability: the enthalpy of the magnesium hydride desorption is  $75 \text{ kJ mol}^{-1}$ ,<sup>[3,4]</sup> that is, relatively high temperatures of 280–300 °C are required for its decomposition. There are several basic strategies aiming to improve the adsorption–desorption kinetics:<sup>[5]</sup> alloying magnesium with transition or rare-earth metals,<sup>[6–8]</sup> adding catalysts to magnesium that accelerate the decomposition of the hydrogen molecule,<sup>[9–11]</sup> and, finally, reduction of the grain size (usage of the nanostructured state).<sup>[5,12–14]</sup> To achieve a synergistic effect, one should combine several approaches simultaneously, for example, use nanostructured magnesium with the addition of a nanosized catalyst. One of the most effective catalysts is a niobium oxide;<sup>[15,16]</sup> moreover, in a case of nanosized niobium oxide, its catalytic

and metallic magnesium. Such structures are obtained by sequential deposition of metallic magnesium and niobium oxide, which prevents the magnesium oxidation despite its high chemical activity. It was shown<sup>[18]</sup> that oxidation of the magnesium layers in  $\text{Mg}/\text{Nb}_2\text{O}_5$  multilayer structure obtained by sequential deposition of  $\text{Nb}_2\text{O}_5$  and Mg was insignificant. The presented results indicated that multilayer films exhibited good hydrogen sorption/desorption kinetics and relatively low desorption temperature.<sup>[18]</sup> However, the thickness of the magnesium layers in the described structures is quite large (50–70 nm)<sup>[18]</sup> and such thickness, from the point of view of the size effect manifestation, is not optimal. Besides that in a case of relatively thick layers, the nanopump effect that draws in and retains hydrogen atoms in a multilayer nanostructure will not be realized.<sup>[21]</sup> We guess that the multilayer nanostructures with magnesium layer thicknesses not exceeding several nanometers are more preferable for hydrogen adsorption.

Such multilayer  $\text{Mg}/\text{NbO}$  nanostructures with magnesium layers thickness of 1–5 nm were obtained in our previous work.<sup>[26]</sup> Despite the partial oxidation of the magnesium layers, the presence of the metallic magnesium phase was observed in the obtained multilayers by X-ray diffraction (XRD) analysis. The magnesium layers with small thickness were not continuous but were discrete, that is, they consisted of nanosized magnesium particles layered distributed in the niobium oxide. We believe that such structure is optimal for hydrogen adsorption because it contains both a hydride-forming metal (Mg) and a catalyst (NbO) in a nanostructured state, as well as a layered distribution of these phases. However, hydrogen sorption/desorption processes require thermal activation, while multilayer nanostructures have relatively low thermal stability. The problem is that

O. Stognei, A. Smirnov, A. Sitnikov  
Department of Solid State Electronics  
Voronezh State Technical University  
Voronezh 394026, Russia  
E-mail: sto.sci.vrn@gmail.com

M. Volochaev  
Institute of Physics by L.V. Kirensky  
Siberian Branch of the Russian Academy of Sciences  
Krasnoyarsk 660036, Russia

 The ORCID identification number(s) for the author(s) of this article can be found under <https://doi.org/10.1002/pssa.202400244>.

DOI: 10.1002/pssa.202400244

when the multilayer nanostructures are being heated, the interfacial interaction or magnesium oxidation begins. For example, in multilayer Mg/Ni systems, the formation of the  $Mg_2Ni$  compound was observed already upon vacuum heating to 50 °C, although the layered structure remained up to 200 °C, despite the interfacial interaction.<sup>[27]</sup> When a similar multilayer is heated in hydrogen environment, the  $Mg_2NiH_4$  compound is observed at 260 °C but after 3 h of annealing under the same conditions the partial oxidation of magnesium occurs.<sup>[22]</sup> Heating the Mg/Pd multilayer structure in hydrogen up to 200 °C initiates interfacial interaction and formation of the  $Mg_xPd_y$  compound.<sup>[23]</sup> The addition of titanium barrier layers separating Mg and Pd was the solution of the problem and also led to increase in the absorption capacities of the multilayers.<sup>[23]</sup> The Mg/SiC multilayer structure showed stability up to 200 °C (in vacuum); however, in the range of 350–400 °C, the interfacial interaction began and formation of the magnesium silicide has occurred.<sup>[28]</sup> In a case of multilayer Mg/ $Nb_2O_5$  structures, heating up to 200 °C, carried out during the magnesium hydrogenation, led to its partial oxidation despite the hydrogen environment.<sup>[18]</sup> Thus, it is obvious that heating of a multilayer structure containing magnesium leads to a chemical interaction between neighbor layers. In the above examples, the thickness of magnesium layers in the multilayer systems varied from 24<sup>[27]</sup> to 730 nm.<sup>[22]</sup> In our opinion, an important question is whether the metallic magnesium phase will be retained when a multilayer structure is heated if the thickness of the layers is only several nanometers. Therefore, the aim of the present work was the investigation of the thermal annealing effect on the multilayer Mg/NbO nanostructure with extremely thin Mg layers (several nanometers). Besides that, influence of the magnesium layers thickness on the phase transformations in the multilayers subjected to thermal annealing was studied. As far as we know, such studies have not been carried out previously within the same system (the same elemental composition, but different layer thicknesses).

## 2. Results and Discussion

The multilayer nature of the obtained samples was confirmed previously by small-angle X-ray reflectometry data and TEM (Figure 1).<sup>[26]</sup> Based on the small-angle reflectometry data, it has been estimated that the average value of one bilayer (Mg +  $NbO_x$ ) thickness in the samples rises from 2.2 to 6.2 nm. The obtained values of the bilayer thickness are in a good agreement with the direct TEM data (Figure 1). It has been also discovered that despite the separate deposition of Mg and  $NbO_x$  layers, the magnesium phase was partly oxidized.<sup>[26]</sup> According to the XRD, only the surface of the magnesium phase was oxidized without penetration of the oxygen atoms into the depth. All samples were obtained under the same conditions; therefore, the thickness of the formed oxide layer is the same. In other words, at the minimum bilayer thickness the Mg is probably oxidized completely but increasing of the magnesium layers thickness (when the bilayer thickness becomes more than 3.3 nm) leads to appearance and increase of the unoxidized part of the Mg phase.

One of the goals of this study was the obtaining a structure where the magnesium phase would be in the form of nanoscale areas. To achieve this aim, the screen with a V-shaped window placed between the magnesium target and substrate holder was used during preparation of the  $(Mg/NbO_x)_{82}$  multilayers. The V-shaped window usage allowed varying the magnesium layers thickness and as a consequence changing their morphology. It has been established previously that the magnesium layers in the  $(Mg/NbO_x)_{82}$  structures are not continuous and are formed from discrete nanosized regions when the bilayer thickness is less than 3.8 nm.<sup>[26]</sup> The continuous magnesium layers are formed when the bilayer thickness exceeds 4.5 nm. Figure 2 presents the  $(Mg/NbO_x)_{82}$  samples resistance versus the nominal thickness of one bilayer as well as the supposed morphology of the multilayers with discrete and continuous Mg layers. In a

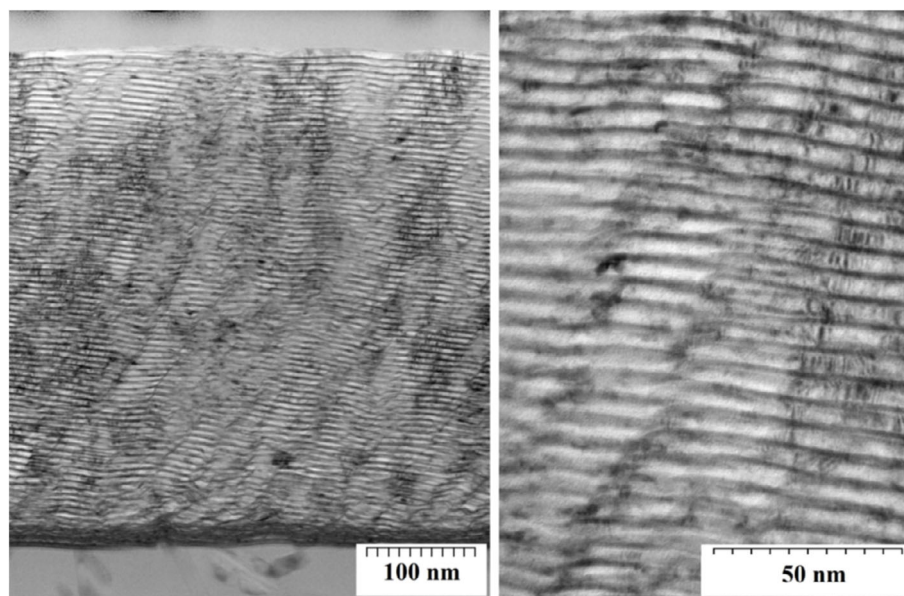


**Figure 1.** TEM images of the cross section of the  $(Mg/NbO_x)_{82}$  multilayer sample with large magnesium layer thickness (estimated bilayer thickness is 6.1 nm). The left and right images were obtained for the same sample but have made with different magnification.

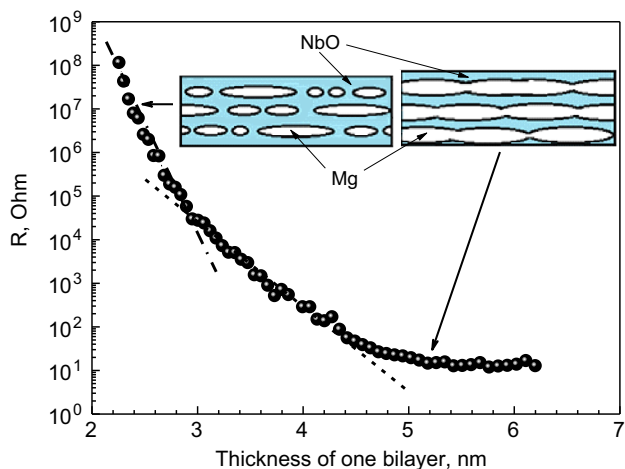


**Figure 2.** Dependence of the electrical resistance of the  $(\text{Mg}/\text{NbO}_x)_{82}$  multilayer nanostructure on the bilayer thickness. The insets show the proposed morphology of the multilayer samples with discreet and continuous magnesium layers.

case of discrete Mg layers, the structure resistance depends exponentially on the geometric parameter (the layer thickness in our case) as it takes place in the granular nanocomposites.<sup>[29]</sup> On the other hand, when the Mg layers are continuous, the structure resistance is practically independent on the layer thickness.

Difference in the magnesium layers morphology affects the processes occurring during the heating of the  $(\text{Mg}/\text{NbO}_x)_{82}$  multilayer structures. The obtained dependencies can be divided into two groups (**Figure 3**). The first one includes samples with a relatively small bilayer thickness. The temperature dependence of the resistance in these samples is similar to the temperature dependence of metal–dielectric composites with nonpercolated structure.<sup>[30]</sup> The composites’ resistance monotonically decreases while they are being heated up to 300–350 °C, and then, with further heating, begins to grow. The resistance decrease in the composites is due to the nonmetallic nature of conductivity (thermoactivated conductivity) and the subsequent increase of the resistance is associated with the “recovery” of the dielectric

matrix structural defects (decrease of its concentration) through which the hopping conduction occurs.<sup>[30]</sup> The same type of the dependencies in composites and in the multilayer structures suggests similar morphology of these objects, which is the discreteness of the magnesium phases.

The resistance change during heating in the second group samples (with large bilayer thickness) differs from the first group samples (**Figure 3a**, samples with the bilayer thickness of 4.7 and 5.5 nm). The samples’ resistance changes slightly when they are being heated up to 440 °C and then there is a sharp resistance increase by 2–2.5 orders and after that, with further heating, the resistance value again changes slightly. This dependence indicates that a certain process begins in the samples at the temperature of 440 °C. It proceeds in a narrow temperature range and leads to a radical change of the electrical resistance. The oxidation of the magnesium layers, which act as conductive channels, can be such a process because the oxidation would obviously lead to a sharp increase of the samples’ resistance. The resistance versus temperature curves of the  $(\text{Mg}/\text{NbO}_x)_{82}$  multilayer samples with the bilayer thickness of 4.7 and 5.5 nm are shown in **Figure 3b,c**. These dependencies allow to see the sign change of the temperature coefficient of resistance (TCR) in the samples. In the initial (low resistance) state, the samples have a positive TCR due to metallic conduction through the continuous magnesium layers.

The sample’s TCR changes the sign from positive to negative after heat to the temperature exceeding the temperature of the sharp resistance increase. The negative TCR sign on the cooling curves is characteristic for the nonmetallic conductivity type. It should be noted that heating and resistance measurements were carried out in a vacuum, so some kind of “internal” source of oxygen is needed for additional oxidation of the magnesium layers. To answer the question what is the source of the additional oxygen, the XRD studies of samples vacuum annealed at a temperature of 450 °C for 2 min were carried out (**Figure 4**). This short-term annealing was chosen to ensure that the structural state of the annealed samples corresponded to the resistance values determined during the resistance measurements.

In the samples with minimum bilayer thickness (minimum thickness of the magnesium layers), the annealing has almost

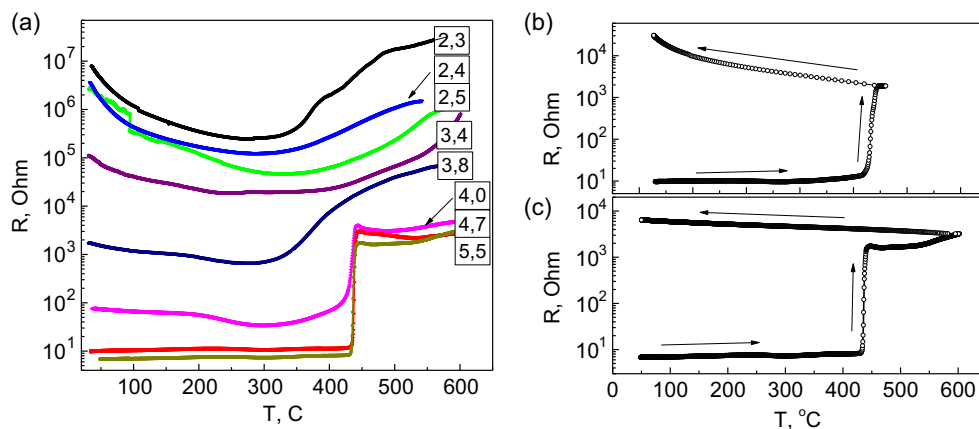


**Figure 3.** a) Temperature dependencies of  $(\text{Mg}/\text{NbO}_x)_{82}$  multilayer resistance with different bilayer thicknesses. The bilayer thickness is given near the curves in nm. The complete temperature dependence of the  $(\text{Mg}/\text{NbO}_x)_{82}$  multilayer resistance with a bilayer thickness of b) 4.7 nm and c) 5.5 nm.

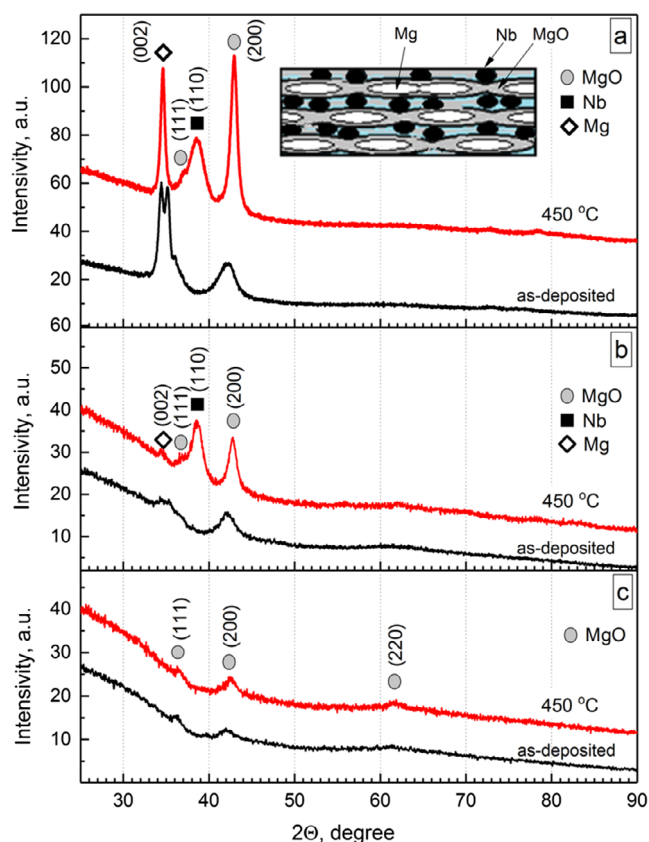


**Figure 4.** XRD of the  $(\text{Mg}/\text{NbO}_x)_{82}$  multilayers in the initial state and after vacuum annealing at 450 °C for 2 min for different bilayer thicknesses: a) 5.5 nm, b) 3.3 nm, and c) 2.5 nm. The inset shows the proposed morphology of the multilayer sample with continuous Mg layers after annealing (rupture of magnesium layers due to oxidation and formation of the metallic niobium phase).

no effect on the diffraction patterns: only peaks of magnesium oxide are present both in the initial state and after the annealing (Figure 4c). One should note that niobium oxide phase in the

obtained multilayers is amorphous, so no diffraction peaks are observed from it. Amorphization of niobium oxide occurs naturally when this material is deposited onto uncooled substrates.<sup>[31–33]</sup> Significantly different behavior is observed in the composites with thicker magnesium layer where the resistance jumps up (Figure 4a,b). First, a peak corresponding to the reflection from the pure crystalline niobium ( $2\theta = 38^\circ$ ) appears on the XRD from the annealed samples. Second, the intensity of the peak of magnesium oxide (200) as well as its shift toward the larger angles increases.

The combination of these facts allows to suggest that during the thermal annealing of the multilayer nanostructures, niobium oxide decomposes with the formation of phase inclusions of pure metal (niobium) while the oxygen released at the decomposing interacts with the magnesium phase, oxidizing it. The shift of the (200) peak from magnesium oxide after annealing may indicate that the oxide composition becomes more stoichiometric due to additional oxidation by the evolving oxygen. In fact, a metallothermic reaction occurs: the reduction of a metal from its compound by another metal, which is chemically much more active than the one being reduced.<sup>[34]</sup> Similar phase transformations with metal reduction from oxide were observed in multilayer metal–oxide structures. For example, the metallothermic reaction occurs during vacuum annealing in of the  $\text{Co}_3\text{O}_4/\text{Zr}$  and  $\text{Co}_3\text{O}_4/\text{Al}$  nanostructures.<sup>[35–37]</sup> The formation of a multilayer structure consisting of cobalt metal granules distributed by layers in a zirconium dioxide or aluminum oxide matrix was a result of the reaction.

One should note that the phase composition of the annealed multilayer structure depends on the bilayer thickness (i.e., thickness of the magnesium layer). The magnesium layers are oxidized almost completely when they have small thickness (the peak of pure magnesium is absent, Figure 4c, or is insignificant in intensity, Figure 4b). The increase of the magnesium layer thickness leads to the fact that the oxygen released during the niobium oxide decomposition is not enough to oxidize the entire thickness of the layer. The large peak corresponding to pure magnesium remains on the XRD curves, although its intensity

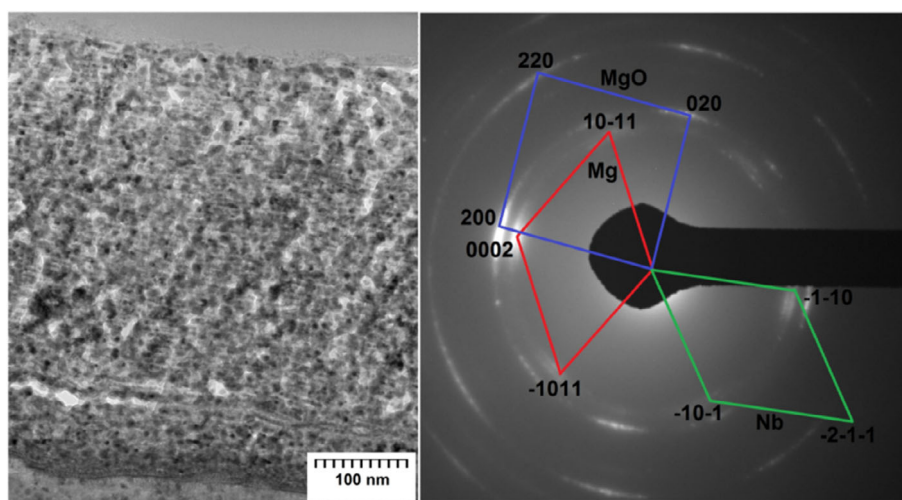


**Figure 5.** TEM image of the cross section of the  $(\text{Mg}/\text{NbO}_x)_{82}$  multilayer sample with large magnesium layer thickness (estimated bilayer thickness is 6.1 nm) after annealing at 450 °C and its electron diffraction pattern.

becomes smaller than the MgO peak (Figure 4a). Annealing also leads to the disappearance of the initial splitting of the magnesium (002) peak and a single, symmetrical maximum is present on the diffraction patterns. The formation of a pure niobium phase as a result of annealing is also confirmed by the TEM data (Figure 5).

Despite the presence of niobium metal and magnesium metal phases in the annealed multilayer structure (Figure 4a), its electrical resistance is two orders of magnitude higher than in the initial state (Figure 3). It is quite understandable. The sharp resistance rise is due to the fact that these metal phases are not continuous after annealing. The continuous magnesium layers are broken by the oxidation while pure niobium forms discrete particles as it usually happens at a metallothermic reaction.<sup>[35–37]</sup> Destruction of the continuous layers is clearly visible on the micrograph of the (Mg/NbO<sub>x</sub>)<sub>82</sub> multilayer structure annealed at 450 °C (Figure 5). The annealing at least leads to rupture of continuous layers, although the layered arrangement of the phase inclusions is retained.

### 3. Conclusion

Sequential deposition of Nb<sub>2</sub>O<sub>5</sub> and Mg thin (few nanometers) layers makes it possible to form multilayer nanostructures with the nanosized magnesium layers. The morphology of the magnesium layers depends on their thickness: the thin layers are discrete (nanosized Mg particles are distributed in niobium oxide) while more thick layers are continuous.

A metallothermic reaction occurs in the multilayer (Mg/NbO<sub>x</sub>)<sub>82</sub> nanostructures during heat treatment. As a result of the reaction, niobium oxide is destroyed, nanosized inclusions of pure niobium are formed, and magnesium layers are additionally oxidized. The additional Mg oxidation leads to breaking of the conductive magnesium layers and, as a consequence, to a sharp increase of electrical resistance of the whole (Mg/NbO<sub>x</sub>)<sub>82</sub> multilayer structure by 2–2.5 orders of magnitude. The rupture of the magnesium layers occurs in the temperature range of 420–440 °C.

Despite the magnesium layer oxidation occurring during a heat treatment, the nanosized metal magnesium regions remain in the volume of the nanostructure if the bilayer thickness is larger than 5.5 nm (the thickness of the single magnesium layer is larger than 4.5 nm). Perhaps it is due to the fact that initially the thicknesses of the metal and oxide layers differ greatly in the studied structures. Thickness of the magnesium layers is several times greater than the thickness of the niobium oxide layers. Therefore, there is not enough oxygen for complete oxidation of the magnesium phase after decomposition of the thin niobium oxide layers. Thus, despite the high chemical activity, nanosized magnesium inclusions can remain unoxidized in (Mg/NbO<sub>x</sub>)<sub>82</sub> nanostructures at least up to a temperature of 450 °C. This makes it possible to use such structures as a material for hydrogen adsorption.

### 4. Experimental Section

The objects of the investigation were samples of a multilayer Mg/NbO<sub>x</sub> nanostructure, differing from each other by the magnesium layer

thickness. The thickness of all Mg layers was the same in certain sample but it was varying from sample to sample. All the (Mg/NbO<sub>x</sub>)<sub>82</sub> multilayer samples were obtained in a single deposition process under the same conditions. The deposition was carried out on substrates which were being moved around two targets (metal and oxide one); thus, the successive deposition of metal and oxide layers has been fulfilled. During the total deposition time, the substrates have made 82 revolutions around the targets; therefore, the obtained multilayer structure consists of 82 bilayers (Mg + NbO<sub>x</sub>). The atomic beam from the sputtering oxide target was directly transferred to the surface of the substrate/multilayer structure, while a screen with a V-shaped window was mounted between the magnesium target and the substrates. This window limited the intensity of the magnesium atom beam condensing onto the surface of the forming structure. Depending on the substrate position relative to the V-shaped window (opposite the wide or narrow part of it), the total number of magnesium atoms condensing onto the substrate was different. Due to the use of such V-shaped window, the deposited multilayer samples differ from each other in the thickness of magnesium layers, while the thickness of niobium oxide layers is constant. The thickness of the niobium oxide layers, estimated on the basis of small-angle X-ray reflection results,<sup>[26]</sup> is 0.96 nm.

The oxide target was fabricated by ceramic technology from Nb<sub>2</sub>O<sub>5</sub> powder with a purity of 99.99%; the magnesium target was made from a cast ingot with a purity of 99.96%. The targets were sputtered by ion-beam sputtering in an argon atmosphere. Previously, the vacuum chamber was evacuated to a pressure of  $4 \times 10^{-6}$  Torr, and then 99.998% purity argon was let into the chamber. The working pressure of the gas was  $7 \times 10^{-4}$  Torr. Each target was sputtered by two serial connected ion sources: the magnesium was sputtered by 80 mA ion current and an accelerating voltage of 1.8 kV; the oxide target was sputtered by an ion current of 70 mA at a voltage of 2.4 kV. Directly before the deposition process, first the targets and then the substrates were cleaned by ion-beam treated, which was carried out at argon operating pressure of  $7 \times 10^{-4}$  Torr. The duration of each target and substrates cleaning was 15 min (45 min in total). The size of the target sputtering surface was 280 × 60 mm, one sample size was 10 × 3 mm, and the distance between the target and the substrates in the deposition sector was 100 mm. Such geometry ensured the uniform thickness of the layers. Sputtering of the targets was carried out continuously while deposition onto substrates was not continuous. The spatial sector within which each target was being sputtered was limited by screens and was equal to 45°. The substrates made a complete revolution around the targets in 263 s; therefore, the deposition time of one layer (metal or oxide) was only 33 s while the substrates were moving within this sector. After deposition of one layer, the substrates kept moving without the material deposition for 98 s (they moved toward the sector of another sputtering target). The next layer was deposited for 33 s in the next sector. The total time of the samples deposition process was 360 min. The deposition was carried out on glass and ceramic (sital) substrates for structural and resistive investigations, respectively.

The structure of the samples was studied by XRD analysis (D2 Phazer diffractometer in Bragg–Brentano geometry; wavelength was 1.541 Å) and high-resolution transmission electron microscopy (TEM) (Hitachi HT7700, accelerating voltage 100 kV). Samples were thinned by ion beam technique (FIB, Hitachi FB2100). The electrical properties of multilayer samples were studied by the two-probe potentiometric method. The probes were placed on the upper surface of the multilayer structure and the current was passed parallel to the layers. Annealing of the samples and the measurement of the temperature dependence of the samples resistance during heating were carried out in a vacuum chamber with a residual pressure of  $1 \times 10^{-4}$  Torr.

### Acknowledgements

This work was supported by the Ministry of Science and Higher Education of the Russian Federation of the state task (grant no. FZGM-2023-0006).

## Conflict of Interest

The authors declare no conflict of interest.

## Data Availability Statement

The data that support the findings of this study are available from the corresponding author upon reasonable request.

## Keywords

electrical transport, hydrogen absorbing materials, multilayers, nanostructured materials, vapor deposition, X-ray diffraction

Received: March 10, 2024

Revised: July 24, 2024

Published online:

- [1] X. Yu, Z. Tang, D. Sun, L. Ouyang, M. Zhu, *Prog. Mater. Sci.* **2017**, *88*, 1.
- [2] I. P. Jain, C. Lal, A. Jain, *Int. J. Hydrogen Energy* **2010**, *35*, 5133.
- [3] Y. Shimizu, M. Otowaki, K. Shirai, M. Ohyanagi, *J. Alloys Compd.* **2019**, *811*, 152062.
- [4] H. Yong, X. Wei, J. Hu, Z. Yuan, M. Wu, D. Zhao, Y. Zhang, *Renewable Energy* **2020**, *162*, 2153.
- [5] X. Ding, R. Chen, J. Zhang, W. Cao, Y. Su, J. Guo, *J. Alloys Compd.* **2022**, *897*, 163137.
- [6] T. Yang, Q. Li, N. Liu, C. Liang, F. Yin, Y. Zhang, *J. Power Sources* **2018**, *378*, 636.
- [7] R. Chen, X. Ding, X. Chen, X. Li, J. Guo, Y. Su, H. Ding, H. Fu, *J. Power Sources* **2018**, *401*, 186.
- [8] J. Zou, H. Guo, X. Zeng, S. Zhou, X. Chen, W. Ding, *Int. J. Hydrogen Energy* **2013**, *38*, 8852.
- [9] S. Milošević, S. Kurko, L. Pasquini, L. Matović, R. Vujasin, N. Novaković, J. G. Novaković, *J. Power Sources* **2016**, *307*, 481.
- [10] G. Barkhordarian, T. Klassen, R. Bormann, *Scr. Mater.* **2003**, *49*, 213.
- [11] O. Friedrichs, F. Aguey-Zinsou, J. R. Ares Fernández, J. C. Sánchez-López, A. Justo, T. Klassen, R. Bormann, A. Fernandez, *Scr. Mater.* **2006**, *54*, 105.
- [12] R. A. Varin, T. Czujko, Z. Wronski, *Nanotechnology* **2006**, *17*, 3856.
- [13] X. Yao, Z. H. Zhu, H. M. Cheng, G. Q. Lu, *J. Mater. Res.* **2008**, *23*, 336.
- [14] Y. Zhao, M. Zhang, Y. Guo, G. Zhu, J. Zhang, X. Guo, X. Zuo, H. Zhao, D. Tang, *Rare Met. Mater. Eng.* **2021**, *50*, 1999.
- [15] G. Barkhordarian, T. Klassen, R. Bormann, *J. Phys. Chem. B* **2006**, *110*, 11020.
- [16] N. Hanada, T. Ichikawa, S. Hino, H. Fujii, *J. Alloys Compd.* **2006**, *420*, 46.
- [17] X. Zhang, X. Zhang, L. Zhang, Z. Huang, L. Yang, M. Gao, C. Gu, W. Sun, H. Pan, Y. Liu, *ACS Appl. Nano Mater.* **2023**, *6*, 14527.
- [18] L. Jiangwen, F. Yiyuan, H. Wencheng, H. Wang, L. Ouyang, M. Zeng, M. Zhu, *J. Phys. Chem.* **2020**, *124*, 6571.
- [19] S. Kumar, Y. Kojima, G. K. Dey, *Int. J. Hydrogen Energy* **2018**, *43*, 809.
- [20] M. S. El-Eskandarany, E. Al-Nasrallah, M. Banyan, F. Al-Ajmi, *Int. J. Hydrogen Energy* **2018**, *43*, 23382.
- [21] M. M. Rampai, C. B. Mtshali, N. S. Seroka, L. Khotseng, *RSC Adv.* **2024**, *14*, 6699.
- [22] S. Ye, L. Ouyang, M. Zhu, *Rare Met.* **2006**, *25*, 295.
- [23] H. Jung, J. Yuh, S. Cho, W. Lee, *J. Alloys Compd.* **2014**, *601*, 63.
- [24] Z. Tarnawski, N. T. Kim-Ngan, K. Zakrzewska, K. Drogowska, A. Brudnik, A. G. Balogh, R. Kužel, L. Havela, V. Sechovsky, *Adv. Nat. Sci.: Nanosci. Nanotechnol.* **2013**, *4*, 025004.
- [25] H. Jung, S. Cho, W. Lee, *Appl. Phys. Lett.* **2015**, *106*, 193.
- [26] O. V. Stognei, A. N. Smirnov, A. V. Sitnikov, K. I. Semenenko, *Solid State Commun.* **2021**, *330*, 114251.
- [27] K. Tanaka, H. Tanaka, H. Kawaguchi, *J. Alloys Compd.* **2002**, *330–332*, 256.
- [28] H. Maury, P. Jonnard, K. Le Guen, J.-M. André, Z. Wang, J. Zhu, J. Dong, Z. Zhang, F. Bridou, F. Delmotte, C. Hecquet, N. Mahne, A. Giglia, S. Nannarone, *Eur. Phys. J. B* **2008**, *64*, 193.
- [29] B. Abeles, P. Sheng, M. D. Coutts, Y. Arie, *Adv. Phys.* **1975**, *24*, 407.
- [30] O. V. Stognei, V. A. Slyusarev, Y. E. Kalinin, A. V. Sitnikov, M. N. Kopitin, *Microelectron. Eng.* **2003**, *69*, 476.
- [31] G. Ramírez, S. E. Rodil, S. Muhl, D. Turcio-Ortega, J. J. Olaya, M. Rivera, E. Camps, L. Escobar-Alarcón, *J. Non-Cryst. Solids* **2010**, *356*, 2714.
- [32] K. I. Semenenko, M. A. Kashirin, O. V. Stognei, A. D. Al-Maliki, *J. Surf. Invest.: X-Ray, Synchrotron Neutron Tech.* **2016**, *10*, 1087.
- [33] C. Nico, T. Monteiro, M. P. F. Graça, *Prog. Mater. Sci.* **2016**, *80*, 1.
- [34] L. L. Wang, Z. A. Munir, Y. M. Maximov, *J. Mater. Sci.* **1993**, *28*, 3693.
- [35] V. G. Myagkov, V. S. Zhigalov, L. E. Bykova, S. M. Zharkov, A. A. Matsynin, M. N. Volochaev, I. A. Tambasov, G. N. Bondarenko, *J. Alloys Compd.* **2016**, *665*, 197.
- [36] V. G. Myagkov, L. E. Bykova, V. S. Zhigalov, A. A. Matsynin, M. N. Volochaev, I. A. Tambasov, Y. L. Mikhlin, G. N. Bondarenko, *J. Alloys Compd.* **2017**, *724*, 820.
- [37] M. N. Volochaev, S. V. Komogortsev, V. G. Myagkov, L. E. Bykova, V. S. Zhigalov, N. P. Shestakov, D. A. Velikanov, D. A. Smolyakov, A. V. Luk'Yanenko, V. B. Rachev, Y. Y. Loginov, I. A. Tambasov, A. A. Matsynin, *Phys. Solid State* **2018**, *60*, 1425.